ELSEVIER

www.elsevier.com/locate/ica
Inorganica Chimica Acta 326 (2001) 89–100

Inorganica Chimica Acta

Metamagnetism in linear chain electron-transfer salts based on decamethylferrocenium and metal–bis(dichalcogenate) acceptors

S. Rabaça [a], R. Meira [a], L.C.J. Pereira [a], M. Teresa Duarte [b], J.J. Novoa [c], V. Gama [a,*]

[a] *Departamento Química, Instituto Tecnológico e Nuclear, P-2686-953 Sacavém, Portugal*
[b] *Departamento Engenharia Química, Instituto Superior Técnico, P-1049-001 Lisbon, Portugal*
[c] *Departamento Química Física and CER Quimica Teórica, Universidad de Barcelona, Av. Diagonal 647, 08028 Barcelona, Spain*

Received 15 May 2001; accepted 12 September 2001

In memory of Professor Olivier Kahn

Abstract

The crystal structure of the electron-transfer (ET) salts $[Fe(Cp^*)_2][M(tds)_2]$, with M = Ni (**1**) and Pt (**2**), consists of an array of parallel alternating donors, $[Fe(Cp^*)_2]^{\bullet+}$, and acceptors, $[M(tds)_2]^{\bullet-}$, ···DADADA···, stacks. For $T > 20$ K, the magnetic susceptibility follows a Curie–Weiss behavior, with θ values of 8.9 and 9.3 K for **1** and **2**, respectively. A metamagnetic behavior was observed in **2**, with $T_N = 3.3$ K and $H_C = 3.95$ kG at 1.7 K, resulting from a high magnetic anisotropy. A systematic study of the intra and interchain magnetic interactions was performed on **1**, **2** and other ET salts based on decamethylferrocenium and on metal–bis(dichalcogenate) acceptors, with a similar crystal structure. The observed magnetic behavior of these compounds is consistent with the presence of strong ferromagnetic intrachain DA interactions and weaker antiferromagnetic interchain interactions, predicted by the McConnell I model. A variety of interionic interchain contacts were found in these ET salts (AA, DD and DA) and these contacts were observed to give rise to antiferromagnetic interchain coupling. Although it was only observed in the case of **2** and $[Fe(Cp^*)_2][Ni(edt)_2]$, metamagnetism is expected to occur at lower temperatures in the other ET salts due to weaker intra and interchain coupling.

Keywords: Magnetic molecular materials; Electron-transfer salts; Crystal structures; Magnetic anisotropy; Metamagnetism; Decamethylferrocenium

1. Introduction

The observation of metamagnetism in the electron-transfer (ET) salt $[Fe(Cp^*)_2]TCNQ$ [1] ($Cp^* = C_5Me_5$, TCNQ = 7,7,8,8-tetracyano-*p*-quinodimethane), with a crystal structure consisting of a parallel arrangement of one-dimensional (1D) chains of alternating donors (D) and acceptors (A), $\cdots D^+A^-D^+A^-\cdots$, in 1979, lead to strong efforts in the search of bulk ferromagnetism in molecule-based ET salts, which was accomplished in 1986 with the report of ferromagnetic (FM) ordering at 4.8 K in $[Fe(Cp^*)_2]TCNE$ [2] (TCNE = tetracyanoethylene). During the following years, five other alternating linear chain decamethylmetallocenium-based ET salts with planar polynitrile acceptors, were reported as ferromagnets, $[M(Cp^*)_2]TCNE$ (M = Mn, [3] Cr [4]) and $[M(Cp^*)_2]TCNQ$ (M = Fe [5], Mn [6], Cr [7]). The study of the relationship between the structure and the magnetic properties in these compounds revealed that the linear alternating chain structural motif clearly favored the existence of FM DA coupling [8]. The first strategy for achieving FM coupling in molecule-based materials was proposed in 1963 [9], the so-called McConnell I mechanism, which, in spite of its simplicity, has shown a good agreement with the experimental observations in these ET salts [10]. However, the magnetic coupling in these ET salts is still a subject of controversy [11], and the validity of the McConnell I mechanism has been put into question based on theoretical arguments [12], and also found not to work in purely organic nitronyl nitroxide crystals [13].

* Corresponding author. Tel.: +351-21-9966 203; fax: +351-21-9941 455.
E-mail address: vascog@itn.pt (V. Gama).

0020-1693/01/$ - see front matter
PII: S0020-1693(01)00669-7

Monoanionic $S = 1/2$ metal–bis(1,2-dichalcogenate) complexes, $[M(X_2C_2R_2)_2]^-$ (M = Ni, Pd and Pt; X = S, Se), have also been used, together with metallocenium donors, in an attempt to obtain new molecule-based magnets. In most cases, the structural motifs obtained differ from the simple alternating linear chain mentioned above, and for a long time that structural DADA motif was observed only in the case of the $[Fe(Cp^*)_2][M(tdt)_2]$ (M = Ni [14], Pt [15]) and $[Mn(Cp^*)_2][M(tdt)_2]$ (M = Ni, Pd, Pt) salts [16]. The magnetic behavior of the linear chain-based ET salts is dominated by DA intrachain FM interactions and in the case of the $[Mn(Cp^*)_2]$ based ET salts metamagnetic behaviors were observed due to a magnetic anisotropy originated by the existence of weak AFM interchain interactions.

The study of alternating linear chain ET salts, based on decamethylmetallocenes and on metalbis(1,2-dichalcogenate) complexes, leads us to conclude that in order to obtain the simple 1D alternating structural motif the dichalcogenate complexes cannot present large dimensions [17]. Seeking to increase the magnetic interactions, in relation to the $[M(tdt)_2]$ based ET salts, we studied decamethylferrocenium salts with other metal–bis(dichalcogenate) acceptors (Scheme 1). Recently we reported a new metamagnet, $[Fe(Cp^*)_2][Ni(edt)_2]$ [17], presenting considerably stronger inter and intrachain magnetic interactions than the $[M(tdt)_2]$ based ET salts. In this case the enhancement of the magnetic interactions is essentially due to the fact that the S and C atoms from the ligand are quite free to interact with the atoms from other ions, due to the absence of the bulky CF_3 groups in the ligand. In the case of $[Fe(Cp^*)_2][Ni(\alpha\text{-tpdt})_2]$ a metamagnetic behavior was observed in agreement with the expected increase in the intrachain interactions [18], which was achieved with the substitution of the two CF_3 groups by a thiophenic ring. In this case a considerable increase of the interchain coupling was expected, due to the presence of the S atoms in the periphery of the ligand. Preliminary results on the replacement of S by Se atoms, through the use of $[Ni(tds)_2]^-$ already indicated the existence of stronger magnetic interactions [19]. The synthesis, crystal structure and magnetic properties of $[Fe(Cp^*)_2][M(tds)_2]$ (M = Ni, **1**, and Pt, **2**) are reported and their behavior is compared with the other linear chain decamethylferrocenium-based ET salts in the perspective of the McConnell I mechanism. In view of the controversy regarding this model, it is interesting to investigate if the McConnell-I model works in these $[Fe(Cp^*)_2]$ based compounds.

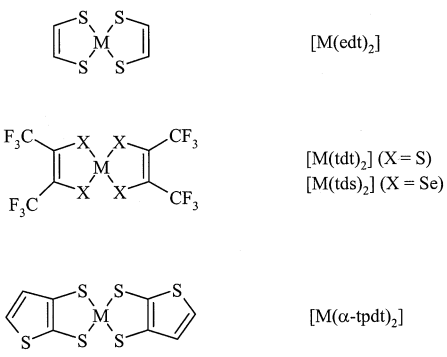

Scheme 1. Metal–bis(dichalcogenate) acceptors.

2. Experimental

2.1. General remarks

$[Fe(Cp^*)_2]BF_4$ was obtained from decamethylferrocene (Aldrich), following literature procedures [20]. The $(n\text{-}Bu_4N)[Ni(tds)_2]$ and $(n\text{-}Bu_4N)[Pt(tds)_2]$ salts were prepared by published literature procedures [21]. Acetonitrile and dichloromethane were distilled under nitrogen over P_2O_5; methanol, ethanol and isobutyl alcohol were distilled under nitrogen from the corresponding magnesium alkoxides. The solvents were deaerated either by successive alternated freezing and evacuating cycles or by bubbling argon for approximately half an hour. All syntheses and manipulations were carried out under nitrogen or argon, in gloveboxes or using Schlenk techniques. Elemental analyses were carried out in a Carlo Erba (EA 1110-CHNS-O).

2.2. $[Fe(Cp^*)_2][Ni(tds)_2]$ (**1**)

This compound was obtained from the mixing of 13.1 mg (0.032 mmol) of $[Fe(Cp^*)_2]BF_4$, dissolved in 2 ml of acetonitrile, with 27.5 mg (0.029 mmol) of $(n\text{-}Bu_4N)[Ni(tds)_2]$ dissolved in 10 ml of methanol. The solution was concentrated with a nitrogen stream (to ca. 7 ml), at room temperature (r.t.), for approximately 2 h, and 21.6 mg (0.021 mmol) of the green polycrystalline product was collected by vacuum filtration in 72% yield. $C_{28}H_{30}F_{12}FeNiSe_4$ (MW = 1025) Calc.: C, 32.81, H, 2.95. Found: C, 32.45, H, 3.19%. Crystallization by slow evaporation of dichloromethane/acetonitrile (1:1) concentrated solutions of $[Fe(Cp^*)_2][Ni(tds)_2]$ afforded plate shaped crystals suitable for X-ray diffraction.

2.3. $[Fe(Cp^*)_2][Pt(tds)_2]$ (**2**)

Dark green crystals of this compound were obtained from the mixing of 18.2 mg (0.044 mmol) of $[Fe(Cp^*)_2]BF_4$, dissolved in 1.5 ml of acetonitrile, with 46.8 mg (0.043 mmol) of $(n\text{-}Bu_4N)[Pt(tds)_2]$ dissolved in 7 ml of methanol. After concentrating for 2 h with a nitrogen stream (to ca. 5 ml), 32.7 mg (0.028 mmol) of the crystalline product was collected by vacuum filtra-

Table 1
Crystal data and structure refinement parameters for compounds **1** and **2**

Compound	$[Fe(Cp^*)_2][Ni(tds)_2]$	$[Fe(Cp^*)_2][Pt(tds)_2]$
Empirical formula	$C_{28}H_{30}F_{12}FeNiSe_4$	$C_{28}H_{30}F_{12}FePtSe_4$
Formula weight	1024.92	1161.30
Temperature (K)	293(2)	293(2)
Wavelength (Å)	0.71069	0.71069
Crystal system	triclinic	triclinic
Space group	$P\bar{1}$	$P\bar{1}$
Unit cell dimensions		
a (Å)	8.581(2)	8.606(2)
b (Å)	10.464(2)	10.521(2)
c (Å)	11.132(2)	11.138(3)
α (°)	107.96(2)	108.81(2)
β (°)	103.65(2)	102.89(2)
γ (°)	101.82(2)	101.300(10)
V (Å^3)	881.3(3)	890.5(4)
Z	1	1
D_{calc} (Mg m^{-3})	1.931	2.166
Absorption coefficient (mm^{-1})	5.158	8.500
$F(000)$	496	546
Crystal size (mm)	$0.38 \times 0.22 \times 0.20$	$0.20 \times 0.10 \times 0.05$
Theta range for data collection (°)	2.03–24.95	2.03–24.98
Index ranges	$-10 \le h \le 10$, $-12 \le k \le 12$, $-1 \le l \le 13$	$-9 \le h \le 10$, $-11 \le k \le 12$; $-13 \le l \le 0$
Reflections collected	3596	3281
Independent reflections	3078 [$R_{int} = 0.0541$]	3110 [$R_{int} = 0.0494$]
Reflections observed ($>2\sigma$)	1608	1738
Absorption correction	ψ-scan [25]	ψ-scan [25]
Max. and min. transmission	0.9997 and 0.9510	0.9996 and 0.9136
Refinement method	full-matrix least-squares on F^2	full-matrix least-squares on F^2
Data/restraints/parameters	3078/163/211	3110/175/211
Goodness-of-fit on F^2	1.034	1.046
Final R indices [$I>2\sigma(I)$]	$R_1 = 0.0777$, $wR_2 = 0.1426$	$R_1 = 0.0765$, $wR_2 = 0.1034$
R indices (all data)	$R_1 = 0.1686$, $wR_2 = 0.1752$	$R_1 = 0.1630$, $wR_2 = 0.1303$
Largest difference peak and hole (e Å^{-3})	0.585 and −0.653	0.911 and −1.007

tion in 65% yield. $C_{28}H_{30}F_{12}FePtSe_4$ (MW = 1161) Calc.: C, 28.96; H, 2.60. Found: C, 28.78; H, 2.29%. Crystallization by slow evaporation of acetonitrile/isobutyl alcohol (3:1) concentrated solutions of $[Fe(Cp^*)_2][Pt(tds)_2]$ afforded plate shaped crystals suitable for X-ray diffraction.

2.4. Magnetic characterization

Static magnetic susceptibility data of compounds **1** and **2** polycrystalline samples, using Teflon sample holders, were obtained with an Oxford Instruments Faraday system, between 1.8 and 300 K, with a 70 kG superconducting magnet. Low temperature magnetization data ($T < 30$ K) were obtained with a Quantum Design SQUID (MPS) magnetometer, with a 55 kG superconducting magnet, and also with an Oxford Instruments Magnetometer (MagLab System 2000), with a 120 kG superconducting magnet, using the extraction method ($T > 1.65$ K). Ac susceptibility measurements were also obtained with the MagLab system. Susceptibility and magnetization data were corrected for contributions due to sample holder and core diamagnetism, estimated from the tabulated Pascal constants.

2.5. X-ray crystallographic study

Greenish plate like crystals of **1** ($0.038 \times 0.022 \times 0.020$ mm) and **2** ($0.026 \times 0.013 \times 0.0065$ mm) were selected and mounted in Lindemann capillaries. Data were collected in an Enraf Nonius CAD4 diffractometer, at r.t. using graphite monochromated Mo radiation ($\lambda = 0.71069$ Å), using the ω–2θ scan mode. Unit cell parameters were determined from the setting angles of 25 well-centered reflections ($12 < \theta < 14°$ and $14 < \theta < 16°$, for **1** and **2**, respectively). Orientation and intensity standard reflections were monitored and no decay was detected. Data were corrected for Lorentz and polarization. Absorption was corrected empirically using the ψ-scan mode. Structures were solved by a combination of direct methods and difference Fourier synthesis, and refined by full-matrix least-squares, using SHELXS-97 [22] and SHELXL-97 [23], respectively. Both compounds crystallize in the triclinic space group $P\bar{1}$, the asymmetric unit containing half cationic and anionic molecules as all heavy atoms, Fe, Ni and Pt are located in special positions (center of symmetry). Due to the large thermal parameters found for the F atoms, some restraints were imposed in the anisotropic thermal parameters (using ISOR) and both the C–F and F–F distances were fixed (using DFIX) thus obtaining an optimized overall geometry. All atoms, except H atoms, were refined anisotropically. H atoms were inserted in idealized positions riding on the parent C atoms, with an overall thermal parameter 1.5 times that of the U_{eq} of the parent C atom. All molecular and crystal representations were done with SCHAKAL-97 [24].

Experimental details on data collection, as well as the final R values and the residual electron densities are given in Table 1.

3. Results and discussion

3.1. Synthesis

The addition of concentrated acetonitrile solutions of $[Fe(Cp^*)_2]BF_4$ to concentrated methanol solutions of $(n\text{-}Bu_4N)[Ni(tds)_2]$, and $(n\text{-}Bu_4N)[Pt(tds)_2]$, after concentration, leads to the isolation of crystalline precipitates of $[Fe(Cp^*)_2][M(tds)_2]$, where M = Ni (**1**) and Pt (**2**). Dark green plate-like single crystals were obtained by slow evaporation from concentrated solutions.

3.2. Crystal structures

Compounds **1** and **2** are isostructural and crystallize on the triclinic system. Relevant crystal, data collection and refinement parameters are presented in Table 1. The $[Fe(Cp^*)_2]^+$ donor shows a C_5 local symmetry and the two Cp rings present a staggered conformation. The $[M(tds)_2]^-$ acceptors are planar and have a D_{2h} local symmetry. The bond distances and angles within donor and acceptor molecules were observed to be in the expected ranges.

The crystal structure of the ET salts **1** and **2** consists of an arrangement of parallel 1D chains of alternating donors (D), $[Fe(Cp^*)_2]^+$, and acceptors (A), $[M(tds)_2]^-$, ···DADADA···, similar to that observed in other decamethylmetallocenium ET salts with planar acceptors [8]. In these compounds the stacking axis corresponds to the [001] direction. The stacking arrangement is shown in Fig. 1(a) for compound **2**, the Fe–M intrachain distances, D_{Fe-M}, are reported in Table 2. The metallic element (M = Ni or Pt) from the acceptors sits above the Cp and is slightly shifted off-center. The angles between the stacking axis and the Cp ring, ξ, and the MSe_4 plane, ψ, as well as the dihedral angle between the Cp and the MSe_4 plane, ζ, are summarized in Table 2. Short intrachain DA contacts were observed in these salts, involving M (Ni or Pt) and carbons from the Cp rings from the donors, in particular in the case of the $[Pt(tds)_2]^-$ based compound (**2**) there are contacts (d) shorter than the sum of the van der Waals radii (d_W), $Q_W = d/d_W < 1$, while in case of **1** these contacts are of the order of d_W or slightly larger, as can be seen in Table 2. These contacts, M–Cp, the average distance between the metal and the C atoms from the C5 ring, ⟨MCp⟩, as well as the shortest separation between the Se atoms and the C atoms from the C5 ring, SeCp, are also shown in Table 2, along with the respective Q_W values. The shorter contacts between the Pt and the C5 ring clearly suggest the existence of stronger intrachain DA magnetic interactions in **2** than in the salt based on the $[Ni(tds)_2]^-$ acceptor, **1**.

For both compounds, there are four distinct chains in the unit cell and a view normal to the chains is presented in Fig. 1(b) for compound **2**. In the unit cell

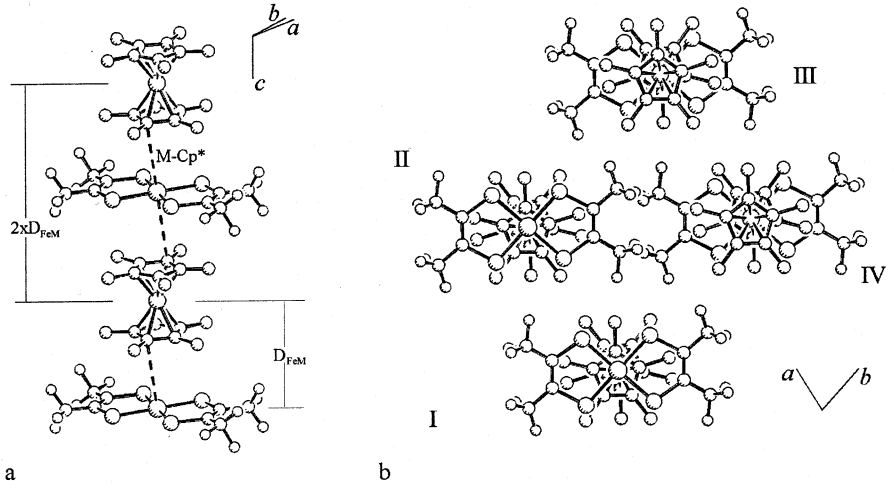

Fig. 1. (a) 1D ···DADADA··· chain in **2**, the thick dashed lines represent the DA Pt–C short contacts. (b) View down the chains (along [001]), showing four chains (I, II, III and IV) for compound **2** (hydrogen atoms were omitted for clarity).

Table 2
Intrachain Fe–M (M = Ni and Pt) distances, D_{Fe-M}. Angles between the stacking axis and the Cp ring, ξ, and the MSe_4 plane, ψ, dihedral angle between the Cp and the MSe_4 plane, ζ. Closest and average intrachain M–Cp contacts. Closest intrachain Se–Cp contact

Compound	D_{Fe-M} (Å)	ξ (°)	ψ (°)	ζ (°)	M–Cp d (Å); Q_W	⟨M–Cp⟩ d (Å); Q_W	Se–Cp d (Å); Q_W
1	5.566	84.32	82.27	2.28	3.844; 1.04	4.070; 1.10	3.845; 1.07
2	5.569	83.73	81.39	3.21	3.826; 0.98	4.070; 1.04	3.877; 1.08

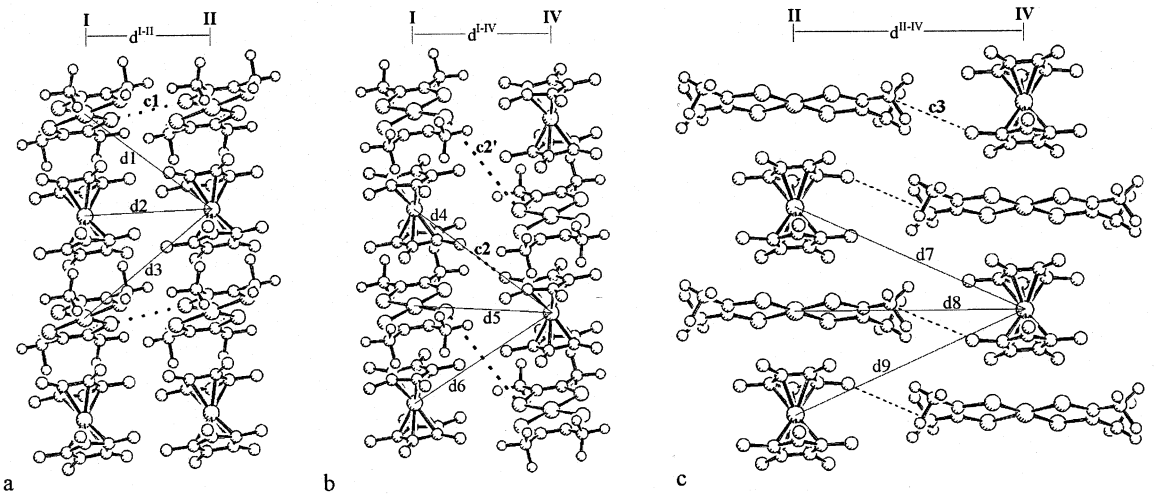

Fig. 2. (a) In-registry arrangement of chains I–II (III–IV) of compound **2**. (b) Out-of-registry arrangement of chains I–IV (II–III) of **2**. (c) Out-of-registry arrangement of chains II–IV of **2**. The solid lines show the closest interchain Fe–Fe, Fe–Pt distances and the thick dotted lines the closest interchain interionic distances (hydrogen atoms were omitted for clarity).

Table 3
Summary of the interchain separations, $d^{X-X'}$, and of the Fe–Fe (M–M) and Fe–M (M = Ni and Pt) interchain distances in compounds **1** and **2**

Compound	d^{I-II} (Å)	d^{I-IV} (Å)	d^{II-IV} (Å)	$d1$ (Å)	$d2$ (Å)	$d3$ (Å)	$d4$ (Å)	$d5$ (Å)	$d6$ (Å)	$d7$ (Å)	$d8$ (Å)	$d9$ (Å)
1	8.338	9.953	10.898	9.059	8.580	11.276	10.463	10.224	12.710	12.097	10.902	12.382
2	8.388	9.958	11.002	9.148	8.605	11.245	10.520	10.194	12.616	12.217	11.005	12.449

three unique interchain arrangements were observed. Chains I–IV and II–IV are out-of-registry, while chains I–II are essentially in-registry. These interchain arrangements are shown in Fig. 2 again for compound **2**. For the compounds under study, the chains in the pairs I–II, I–IV and II–IV are symmetry related by inversion centers. Table 3 summarizes the interchain distances, $d^{X-X'}$, as well as the shortest Fe–M and Fe–Fe (M–M) interchain separations, dx. No interchain contacts shorter than the sum of the van der Waals radii were found. The shortest interchain interionic distances, **cx**, are shown in Fig. 2, for each interchain arrangement. In the I–II pair, **c1** refers to (AA) Se–Se contacts, of 4.582 and 4.348 Å (or $Q_W = 1.15$ and 1.09), for **1** and **2**, respectively. In case of the pair I–IV, **c2** refers to (DD) C–C contacts, from the Me groups, with values of 4.215 and 4.263 Å ($Q_W = 1.32$ and 1.33) for **1** and **2**, respectively. In this pair a longer (AA) Se–Se contact **c2′** is also represented corresponding to distances of 6.698 and 6.640 Å ($Q_W = 1.67$ and 1.66) for **1** and **2**, respectively. For the pair II–IV the shortest contact **c3** refers to (DA) C–C, between a Me and a CF_3, with distances of 4.283 and 4.293 Å ($Q_W = 1.34$) for **1** and **2**, respectively. Contacts involving H or F atoms were not considered to play a significant role on the interchain interactions and were omitted. The arrangements of chains I–II and I–IV are identical to the ones of the chains III–IV and II–III, respectively.

3.3. Magnetic properties

The room temperature effective magnetic moments, μ_{eff}^{RT}, are 3.03 and 3.35 μ_B for **1** and **2**, respectively. A compressed polycrystalline sample was used in the case of **1**, and the experimental value agrees with the calculated, $\mu_{eff}^{calc} = 3.01\ \mu_\beta$. For compound **2**, a free polycrystalline sample was used and the experimental value is slightly larger, which is attributed to orientation effects due to the applied field and the large anisotropy of the g values of the $S = 1/2$ decamethylferrocenium donor [20], $g_\parallel = 4$ and $g_\perp = 1.3$. The temperature dependence of the magnetic susceptibility, χ, for compounds **1** and **2**, was obtained between 1.7 and 300 K, using the Faraday method, with an applied field of 5 kG. The data fit the Curie–Weiss law, $\chi = C/(T - \theta)$, between 20 and 300 K, with positive θ values of 8.9 and 9.3 K for **1** and **2**, respectively, indicating the existence of dominant FM interactions, which are attributed to the intrachain DA interactions. The temperature dependence of the product χT is shown in Fig. 3 for **1** and **2**, at high temperatures, χT increases upon cooling (dominant FM interactions) and presents a maximum at low temperatures in the case of **2**.

In the case of compound **2**, the magnetization temperature dependence, shown in Fig. 4, for low applied magnetic fields shows a maximum at approximately 3.5 K, signaling an AFM phase transition. The maximum

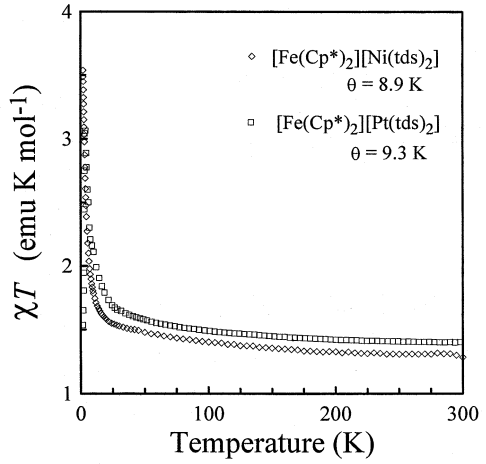

Fig. 3. χT temperature dependence of compounds **1** and **2**, with an applied field of 5 kG.

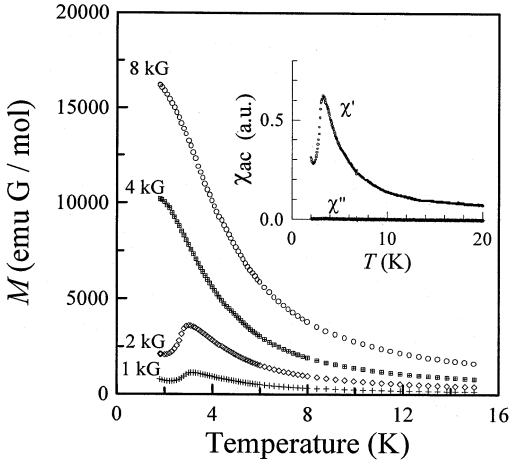

Fig. 4. Magnetization temperature dependence of compound **2**, with applied magnetic fields of 1, 2, 4 and 8 kG. The inset shows the temperature dependence of the real (χ') and imaginary (χ'') parts of χ_{ac}, at low temperatures.

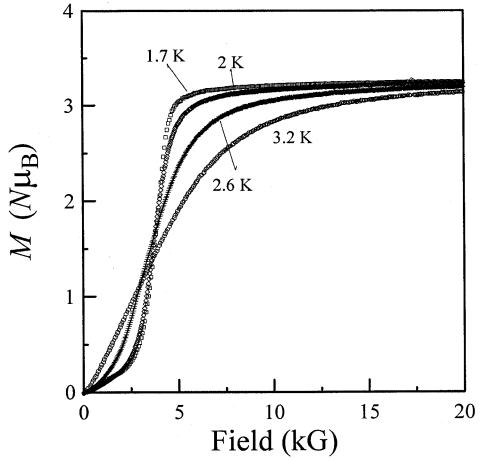

Fig. 5. Magnetization isothermals of compound **2**, at 1.7, 2, 2.6, and 3.2 K.

shifts to lower temperatures with increasing fields and is suppressed for high fields, suggesting the existence of a field induced transition. A T_N value of 3.3 K was obtained from ac susceptibility measurements, through the observation of a maximum in the real part of the ac susceptibility, χ', as shown in the inset of Fig. 4. The magnetization field dependence, together with the magnetic anisotropy, which was expected from the structural analysis, is consistent with a metamagnetic behavior. The magnetization isothermals, shown in Fig. 5, below $T_N = 3.3$ K, present a clear sigmoidal behavior, which is typical of metamagnets for $T < T_N$. At 1.7 K, the magnetization first increases slowly with the applied field, as for an AFM, and increases rapidly, at approximately 3.5 kG, to the high field state, as expected for a metamagnet. At 1.7 K, the critical field, H_C, defined as the maximum in dM/dH, is 3.95 kG. Compound **2** reaches saturation, $M = M_s$, at a relatively low field, $H \approx 5$ kG, unlike other decamethylmetallocenium-based metamagnetic salts, such as [Fe(Cp*)$_2$]TCNQ [1], [Fe(Cp*)$_2$]DMe-DCNQI [26], [Mn(Cp*)$_2$][M(tdt)$_2$] (M = Ni, Pd, Pt) [16] and [Fe(Cp*)$_2$][Ni(edt)$_2$] [17], where saturation occurs at applied magnetic fields much higher than H_C. This effect can be attributed to the relatively strong AFM interchain interactions in this compound. From the magnetization field and temperature dependencies, it was possible to obtain a phase diagram for compound **2**, presented in Fig. 6, where the solid symbols refer to the data obtained from the isothermal measurements and the open symbols refer to the temperature dependence experiments.

The crystal structure of compounds **1** and **2** clearly suggests the existence of a strong DA orbital overlap, considering the short distances between the Cp rings from the donors and the MSe_4 central fragments from the acceptors (where most of the spin density is expected to reside). Besides short contacts were observed to exist essentially in the basic 1D ···DADADA··· structural motif. In this sense the intrachain DA magnetic interactions are expected to be much stronger than the interchain magnetic interactions. Nevertheless if we consider magnetic ordering, the weaker interchain interactions are as important as the intrachain, since the magnetic ordering is a bulk property. For the compounds **1** and **2**, no short interchain contacts ($Q_W \leq 1$) were observed. However, relatively short interchain interionic distances were observed essentially in the pairs I–II, involving AA Se–Se contacts, **c1**, which are only slightly larger than Q_W. These contacts are expected to give rise to significant interactions between the I–II and III–IV pairs in both compounds. According to the McConnell I model, these interactions are predicted to be AFM, as the spin density of both atoms has the same sign, which is consistent with the metamagnetic behavior observed in case of compound **2**. In case of **1**

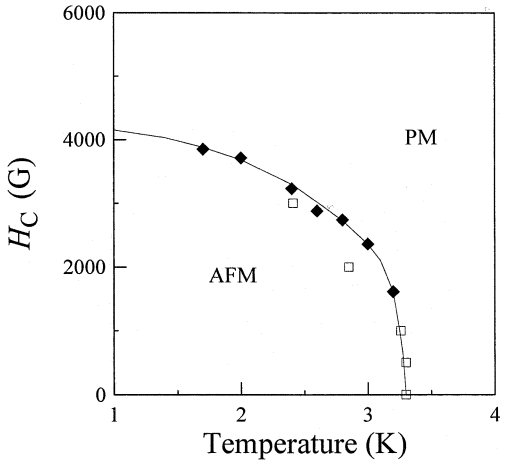

Fig. 6. Magnetic phase diagram of compound **2**. The solid and open symbols refer to the data obtained from the isothermal and isofield measurements, respectively.

a metamagnetic transition is also expected, but in this case the transition temperature must be lower than the minimum value we could achieve (1.7 K). The isostructural Mn analogue of **1**, $[Mn(Cp^*)_2][Ni(tds)_2]$ [19], presents a metamagnetic behavior with $T_N = 2.1$ K, and as $T_N \propto |E_{intra}E_{inter}|^{1/2}$ [16], where E_{intra} is the DA intrachain interaction, $E_{intra} \propto S_D S_A J_{DA}$, and E_{inter} the effective interchain interaction, in case of **1**, T_N is expected to be considerably lower. In the case of **2**, $T_N = 3.3$ K, and a significantly higher Néel temperature was observed in the Mn analogue, $[Mn(Cp^*)_2][Pt(tds)_2]$, $T_N = 5.7$ K [27]. Considering the spin effect observed in the $[Pt(tds)_2]$ compounds a T_N value of the order of 1.2 K is expected in the case of **1**.

3.4. Magnetic coupling

The Curie–Weiss θ values obtained at high temperatures, low temperature ($T > 1.8$ K) magnetic behavior, Néel temperatures, and critical fields for the linear chain ET salts based on decamethylferrocenium and on metal–bis(1,2-dichalcogenate) acceptors, $[Fe(Cp^*)_2][Ni(tds)_2]$ (**1**), $[Fe(Cp^*)_2][Pt(tds)_2]$ (**2**), $[Fe(Cp^*)_2][Pt(tdt)_2]$ (**3**), $[Fe(Cp^*)_2][Ni(edt)_2]$ (**4**), $[Fe(Cp^*)_2][Ni(tdt)_2]$ (**5**) and $[Fe(Cp^*)_2][Ni(\alpha\text{-tpdt})_2]$ (**6**), are compared in Table 4.

Compound **3** is isostructural with **1** and **2**. Although no metamagnetic ordering was reported, in the same way as for compound **1**, a metamagnetic behavior is expected to occur at low temperatures. In compound **3**, short intrachain DA contacts were observed involving the Pt and C atoms from the Cp ring, with Pt–C distances of 3.747 and 3.807 Å ($Q_W = 0.96$ and 0.98), the closest DA S–C distance is 3.715 Å ($Q_W = 1.08$). The interchain arrangements are similar to the ones presented in Fig. 2, and, for the I–II pair, the **c1** (AA) S–S contact, is 4.557 Å ($Q_W = 1.23$). In case of the pair I–IV, **c2** (DD) C–C contacts, from the Me groups, is 4.078 Å ($Q_W = 1.27$) and the (AA) S–S contact **c2′** is 6.497 Å ($Q_W = 1.76$).

A metamagnetic behavior was observed in compound **4** and its crystal structure, as in the case of compounds **1**–**3**, consists of parallel 1D chains of alternating donor, $[Fe(Cp^*)_2]^+$, and acceptor, $[Ni(edt)_2]^-$, ···DADADA···, but a distinct packing arrangement was observed in this compound, which concerns essentially with the interchain arrangements. The chain arrangements of compound **4** are shown in Fig. 7. In this compound, the intrachain arrangement is similar to the one observed in **1**–**3**, where the Ni sits above the Cp ring. In compound **4**, short intrachain DA contacts were observed involving the Ni and one of the C atoms from the Cp ring, with a Ni–C distance of 3.677 Å ($Q_W = 0.99$). A top view of the chains of compound **4** is represented in Fig. 7(a). In the case of **4** the most relevant interchain contacts involve the in-registry pair II–IV, with AA C–C contacts (ethylenic carbons) of 3.507 Å ($Q_W = 1.11$). The out-of-registry pairs I–II and I–IV show a similar interchain arrangement, with DA C–S contacts (C from Me from the donor and a S from the acceptor) of 3.812 Å ($Q_W = 1.11$). These arrangements are shown in Fig. 7(b) and (c).

The same type of crystal structure, based on an arrangement of parallel alternating DA linear chains, is observed in the case of compound **5**, but there are differences in the intra and interchain arrangements. As in case of compounds **1** and **3** no metamagnetic behavior was observed in **5**, down to 1.8 K, but it is expected to occur at lower temperatures, as its isostructural Mn analogue, $[Mn(Cp^*)_2][Ni(tdt)_2]$, presents a metamagnetic transition at $T_N = 2.4$ K [16]. The chain arrangements of compound **5** are shown in Fig. 8. For **5** the 1D

Table 4
Summary of the magnetic behavior of the linear chain ET salts based on decamethylferrocenium and on metal–bis(1,2-dichalcogenate) acceptors

Compound	θ (K)	Low temperature behavior	T_N (K)	H_C (G) (at T (K))	Reference
$[Fe(Cp^*)_2][Ni(tds)_2]$ (**1**)	8.9	PM			this work
$[Fe(Cp^*)_2][Pt(tds)_2]$ (**2**)	9.3	MM	3.3	3950 (1.7)	this work
$[Fe(Cp^*)_2][Pt(tdt)_2]$ (**3**)	27	PM			[15]
$[Fe(Cp^*)_2][Ni(edt)_2]$ (**4**)	−5	MM	4.2	14 000 (1.8)	[17]
$[Fe(Cp^*)_2][Ni(tdt)_2]$ (**5**)	~5–15	PM			[14]
$[Fe(Cp^*)_2][Ni(\alpha\text{-tpdt})_2]$ (**6**)	0	MM	2.6	600 (1.6)	[18]

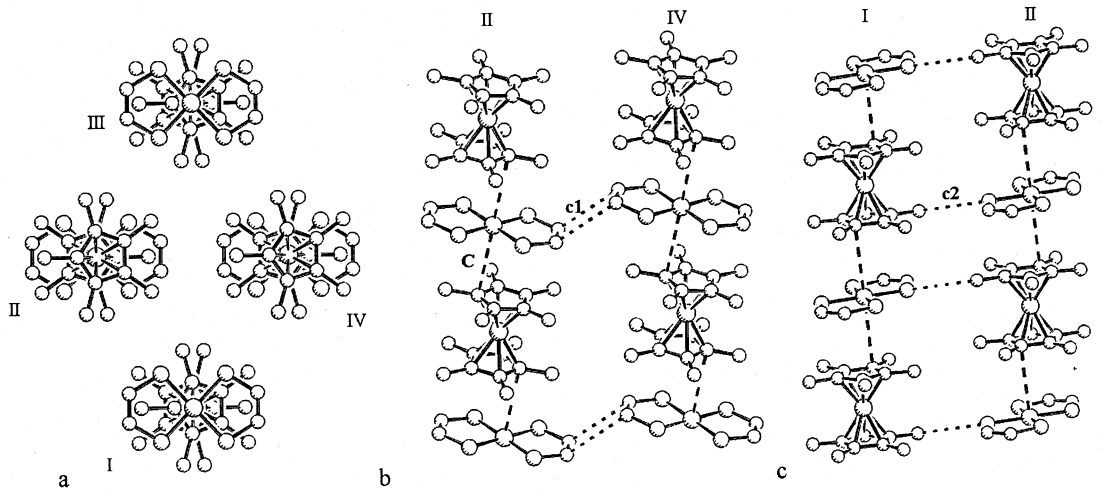

Fig. 7. (a) View parallel to the chains showing four chains in compound **4**. (b) Out-of-registry arrangement of chains II–IV of compound **4**. (c) In-registry arrangement of chains I–II of **4**. The thick dotted lines show the closest interchain interionic distances (hydrogen atoms were omitted for clarity).

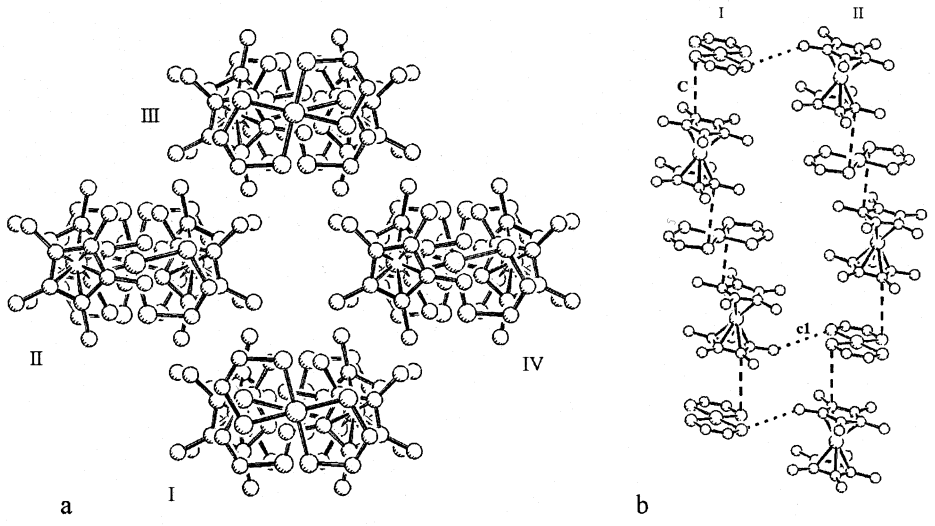

Fig. 8. (a) View parallel to the chains showing four chains in compound **5**. (b) Out-of-registry arrangement of chains I–II of compound **5**. The thick dotted lines show the closest interchain interionic distances (hydrogen atoms and CF_3 groups were omitted for clarity).

DA chains show a zigzag arrangement, where one NiS_2C_2 ring of the acceptor sits above the Cp ring. In this compound, no intrachain DA short contacts were found and the closest interatomic separation between the acceptor and the Cp ring are relative to S–C contacts of 3.946 Å ($Q_W = 1.14$). A top view of the chains of compound **5** is represented in Fig. 8(a). In the case of **5**, for clarity the CF_3 groups were omitted, as the spin density in these fragments is negligible (as will be shown below) and they are not expected to contribute significantly to the magnetic interactions. For compound **5** the most relevant interchain contacts concern the out-of registry pairs I–II and I–IV, these arrangements are similar and the first one is shown in Fig. 8(b). These pairs show interchain DA C–S contacts, involving C atoms from the Me groups of the donors and S atoms of the acceptors. The interatomic distance of these contacts is 3.728 Å ($Q_W = 1.08$).

Although the crystal structure of compound **6** is also based on an alternating DA linear chain motif, it is considerably different from the ones of the previous compounds. In this case the crystal structure consists of layers composed of out-of-registry parallel alternating DA chains. Chains in adjacent layers are nearly perpendicular to each other. A metamagnetic behavior was also observed in this compound, with $T_N = 2.6$ K [18]. Due to the different crystal structures of compound **6** it will not be compared with the other ET salts.

In order to analyze the magnetic coupling in compounds **1** and **2** and compare its magnetic behavior with the other linear chain decamethylferrocenium-based ET salts (**3**–**5**), the spin densities of the donor, $[Fe(Cp^*)_2]$, and several of the metal–bis(dichalcogenate) acceptors were calculated. The atomic spin populations were computed by performing a Mulliken population analysis on the wave function obtained by a B3LYP density functional (gradient-corrected exchange and correlation of Becke) [28] computations using the LANL2DZ basis set [29], in which pseudopotentials are used for the core electrons and a double-zeta basis set is employed for the valence electrons. The geometries used for the molecules were those found in the crystals without further changes. The ground state of all the fragments is a doublet and spin contamination found in the B3LYP wavefunction was always very small. The labeling of the atoms from the donor and acceptor molecules is represented in Fig. 9.

In the case of $[Fe(Cp^*)_2]^+$, most of the spin density resides on the Fe atom ($\rho_{Fe} = 1.26$), resulting from a spin polarization effect the C atoms from the Cp ring (C) present a negative spin density ($\rho_C = -0.03$) and the C atoms from the Me groups (C′) present a small positive spin density ($\rho_{C'} = 0.002$). The spin density found on the H atoms is negligible ($|\rho| < 0.002$). These results are in very good agreements with the NMR experimental results for the $[Fe(Cp^*)_2]^{\bullet +}$ radical [30], and with the experimental ESR results for the $[Ni(tds)_2]^{\bullet -}$ and $[Pt(tds)_2]^{\bullet -}$ radicals [21].

In case of the metal–bis(dichalcogenate) mono anionic complexes most of the spin density resides on the MX_4, X = S or Se, central fragment, and in some cases a small spin density was observed to be located on the ethylenic C atoms from the five-membered rings MX_2C_2. The results of the spin density calculations for these acceptors are presented in Table 5. Once these values are known, according to the McConnell I theory [9], it is possible to determine the nature of the magnetic interaction between two radicals. Since it depends on the shortest contacts between these two radicals and on the sign of the atomic spin population from the two atoms making the shortest contacts. FM interactions are predicted whenever the two atoms making the short contacts have opposite atomic spin populations, while AFM are obtained when the two atoms have the same sign in the atomic spin population. Let us mention again that the basic theory supporting this approximation has been shown to be incorrect in general [12], but we are going to use it to test its validity in this family of ET salts.

The intra and interchain contacts from compounds **1**–**5** are summarized in Table 6, along with the spin densities of the atoms involved in the contacts and the predictions of the nature of the magnetic interactions according to the McConnell I mechanism. In case of the intrachain contacts, DA contacts involving the metallic element and a chalcogen from the acceptor and carbons from the Cp ring (C–M and C–X) are both referred, as those distances are of the same order. It

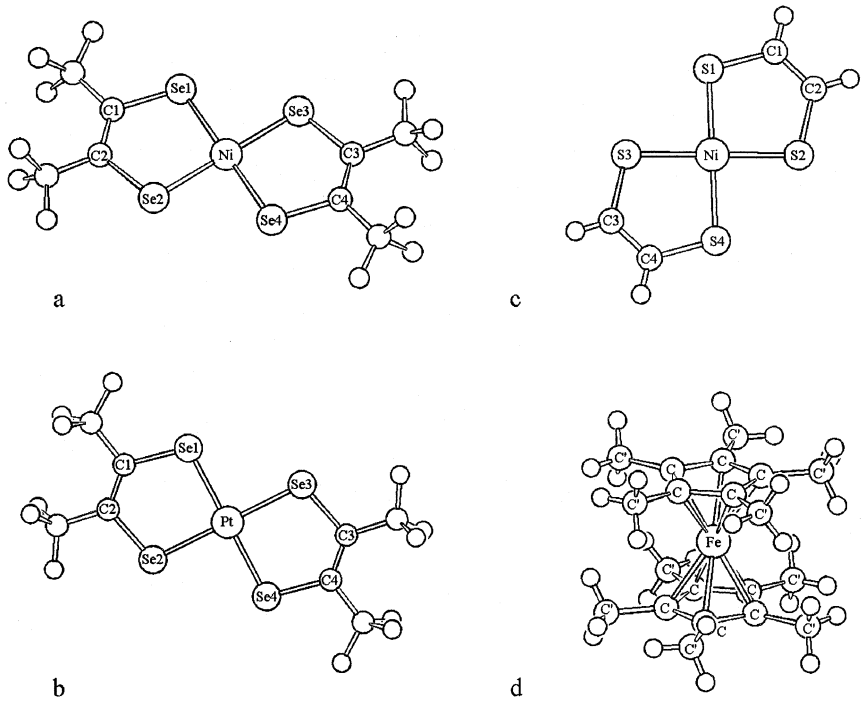

Fig. 9. Schematic representation of the acceptors: (a) $[Ni(tds)_2]^-$ (**Al**); (b) $[Pt(tds)_2]^-$ (**A2**); (c) $[Ni(edt)_2]^-$ (**A4**), and of the donor (d) $[Fe(Cp^*)_2]^+$. The atomic labeling refers only to the atoms with significant spin density ($|\rho| \geq 0.002$).

Table 5
Spin density distribution on the metal–dichalcogenate acceptors of ET salts **1**–**5**

Atom	**A1** [a] $[Ni(tds)_2]^-$	**A2** [a] $[Pt(tds)_2]^-$	**A3** [b] $[Pt(tdt)_2]^-$	**A4** [c] $[Ni(edt)_2]^-$	**A5** [b] $[Ni(tdt)_2]^-$
M	0.170	0.130	0.13	0.120	0.17
X1	0.210	0.230	0.2	0.200	0.2
X2	0.200	0.220	0.2	0.200	0.2
X3	0.180	0.230	0.2	0.200	0.2
X4	0.200	0.220	0.2	0.200	0.2
C1	0.010	[d]		0.030	
C2	0.020	[d]		0.030	
C3	0.020	[d]		0.030	
C4	0.002	[d]		0.030	

[a] Remaining atoms have $|\rho| < 0.002$.
[b] Estimated values based on the ones from **1**, **2**, and **4**.
[c] Remaining atoms have $|\rho| < 0.003$.
[d] $|\rho| < 0.002$.

Table 6
Summary of the intra and interchain shortest contact characteristics of ET salts **1**–**5**. The nature of the interactions, according to the McConnell I model, is also referred (H atoms were neglected as referred in the text)

ET salt	Intrachain				Interchain (**c1**)				Interchain (**c2**)			
	Contact	*d* (Å)	Spin dens.	Int.	Contact	*d* (Å)	Spin dens.	Int.	Contact	*d* (Å)	Spin dens.	Int.
1	DA, C–Ni	3.844	−0.03; 0.17	FM	AA: Se–Se	4.582	0.20; 0.20	AFM	DD: C–C	4.215	0.002; 0.002	AFM
	C–Se	3.845	−0.03; 0.20	FM								
2	DA: C–Pt	3.826	−0.03; 0.127	FM	AA: Se–Se	4.348	0.22; 0.22	AFM	DD: C–C	4.263	0.002; 0.002	AFM
	C–Se	3.877	−0.03; 0.22	FM								
3	DA: C–Pt	3.747	−0.03; 0.13	FM	AA: S–S	4.557	0.20; 0.20	AFM	DD: C–C	4.079	0.002; 0.002	AFM
	C–S	3.715	−0.03; 0.20	FM								
4	DA: C–Ni	3.677	−0.03; 0.12	FM	AA: C–C	3.507	0.03; 0.03	AFM	DA: C–S	3.812	0.002; 0.20	AFM
	C–S	3.769	−0.03; 0.20	FM								
5	DA: C–Ni	4.119	−0.03; 0.17	FM	DA: C–S	3.728	0.003; 0.20	AFM	DA: C–S	3.728	0.002; 0.20	AFM
	C–S	3.946	−0.03; 0.20	FM								

must be noted that, in all cases, the shortest interchain contacts involve H or F atoms (not referred so far) and these types of contacts were neglected, according to the strict application of the McConnell I mechanism, this would lead to very weak magnetic interactions since the spin density on these atoms is expected to be very small. With these limitations this analysis predicts the existence of FM intrachain interactions and AFM interchain interactions. This result supports the existence of a strong magnetic anisotropy in these compounds and is consistent with the observation of metamagnetism in compounds **2** and **4**.

The positive spin density on the atoms from the MX_4 fragment and the negative spin density on the Cp ring are expected to give rise to an intrachain FM coupling, according to the McConnell I mechanism. The intrachain coupling is expected to be strong especially in the case of compounds **2**–**4**, where there are contacts inferior than the sum of the van der Waals radii. In case of **1** the DA interatomic distances are slightly large and these interactions are expected to be slightly weaker, while for **5** these distances are considerably longer and the intrachain coupling is expected be significantly weaker. Then for these compounds the intrachain magnetic coupling is expected to decrease in the order $\mathbf{2} \approx \mathbf{3} \approx \mathbf{4} > \mathbf{1} > \mathbf{5}$.

A large variety of situations were observed in the interchain interionic contacts. In case of compounds **1**–**3**, the stronger interactions are relative to AA (Se–Se) contacts, **c1**, in arrangement 1 (corresponding to the I–II interchain arrangement shown in Fig. 2(a) and to DD (Me–Me), **c2**, or AA (Se–Se), **c2′**, contacts in arrangement 2 (I–IV interchain arrangement—Fig. 2(b)). For compound **4** the stronger interactions correspond to AA (C–C) contacts, **c1**, in arrangement 1 (II–IV interchain arrangement—Fig. 7(b) and to DA (Me–S), **c2**, contacts in arrangement 2 (I–II interchain arrangement—Fig. 7(c)). In the case of **5**, the stronger

interchain interactions are expected to be related to the DA (Me–S), **c1** and **c2**, contacts, which are alike in both arrangements 1 (I–II interchain arrangement—Fig. 8(b)) and 2 (I–IV interchain arrangement). In spite of the variety of situations observed in the interchain contacts, all the atoms involved have the same sign and, according to the predictions of the McConnell I mechanism, they are expected to give rise to AFM coupling. The spin density calculations and the analysis of the interionic contacts clearly indicate that these ET salts are strongly anisotropic magnetic systems and support the existence of metamagnetism, which could be observed in **2** and **4**. Considering the spin densities and distances of the atoms involved in the interchain contacts it is expected that the magnetic interactions decrease in the order $\mathbf{c1(1-3) > c1(4) > c1(5) = c2(5) \approx c2(4) \gg c2(1-3)}$.

In the case of compounds **4** and **5**, comparing the interionic separations and the spin densities of the atoms involved in the contacts, the interchain magnetic coupling is expected to be considerably weaker than the intrachain and these can be considered quasi-1D magnetic systems. In the case of the isostructural **1**–**3** compounds, quite strong magnetic coupling is expected from the interchain arrangements 1, due to the short Se–Se or S–S contacts (**c1**) and the high spin density on the chalcogen atoms. While in the arrangements 2, the interactions, due to the C–C contacts (**c2**), are expected to be much weaker, and these compounds can be described as quasi-2D magnetic systems. The different dimensionality of these systems can be related to the fast saturation observed in the isothermals, just above H_C, in compound **2**, or in the Mn analogue of **1**, $[Mn(Cp)_2][Ni(tds)_2]$ [19], in clear contrast with compound **4** or the Mn analogue of **5**, $[Mn(Cp)_2][Ni(tdt)_2]$ [16], where saturation occurs only at very high magnetic fields, when the temperature is not much lower than T_N.

In the linear chain $[Fe(Cp^*)]^+$ based compounds, metamagnetism was observed only in compounds **2** and **4**. For the isostructural Mn compounds of **1**, **2** and **5**, metamagnetism was also observed, with $T_N = 2.1$, 5.7 and 2.4 K, respectively, and as $T_N \propto |E_{intra}E_{inter}|^{1/2}$, in case of **1** and **5**, T_N is expected to present similar values, but considerably lower. Admitting that the relation obtained for the intrachain magnetic coupling ($\propto E_{intra}$) is $\mathbf{2 \approx 3 \approx 4 > 1 > 5}$. From the correlation of E_{intra} with the T_N values of **2** and **4** and the Mn analogues of **1**, **2** and **5**, it is possible to conclude that for these compounds, E_{inter} (effective interchain interaction) decreases in the order $\mathbf{4 > 2 > 5 > 1}$. No magnetic transition was reported in case of compound **3** (its Mn analogue is not isostructural), but as the S–S contact must be weaker than the Se–Se contact in **1**, it is reasonable to admit that in **3** the interchain magnetic coupling is weaker than in **1**.

The observed relationship between the E_{inter} in the case of **2** and **4** is consistent with the critical field values in these compounds, $H_C = 3.95$ and 14 kG, as according to an Ising model [31], in metamagnets the critical fields are predicted to be proportional to the interchain exchange constants.

4. Conclusions

One of the main motivations of this study was to achieve stronger magnetic interactions (intra and interchain) in the alternating linear chain based ET salts $[Fe(Cp^*)_2]A$, where the acceptor molecules A are metal–bis(dichalcogenate) complexes. In this case the enhancement of the magnetic interactions was expected to occur through the substitution of S (in $[M(tdt)_2]$, M = Ni, Pt) by Se (in $[M(tds)_2]$, M = Ni, Pt). The study of $[Fe(Cp^*)_2][M(tds)_2]$, M = Ni, Pt, revealed that these are highly anisotropic magnetic systems with strong FM intrachain interactions coexisting with weaker AFM interchain interactions. The magnetic anisotropy is responsible for the observation of metamagnetism in $[Fe(Cp^*)_2][Pt(tds)_2]$, with $T_N = 3.3$ K and $H_C = 3950$ G. No magnetic ordering was observed in case of $[Fe(Cp^*)_2][Ni(tds)_2]$ due to the weaker intra and interchain magnetic interactions.

The analysis of the crystal structures, the magnetic behaviors and spin density calculations of the known ET salts based on decamethylferrocenium and on metal–bis(dichalcogenate) acceptors with structures consisting on arrangements of parallel alternating DA linear chains, $[Fe(Cp^*)_2][Ni(tds)_2]$ (**1**), $[Fe(Cp^*)_2]$-$[Pt(tds)_2]$ (**2**), $[Fe(Cp^*)_2][Pt(tdt)_2]$ (**3**), $[Fe(Cp^*)_2][Ni(edt)_2]$ (**4**) and $[Fe(Cp^*)_2][Ni(tdt)_2]$ (**5**), allowed a systematic study of the intra and interchain magnetic interactions. The analysis of the intrachain contacts in the perspective of the McConnell I mechanism suggests the existence of intrachain FM coupling, which shows a good agreement with the experimental observations. The intrachain magnetic coupling is estimated to decrease in the order $\mathbf{2 \approx 3 \approx 4 > 1 > 5}$. A variety of interionic interchain contacts were observed in these ET salts, AA (Se–Se in **1** and **2**, S–S in **3**, and C–C in **4**), DD (Me–Me in **1**, **2** and **3**) and DA (Me–S in **4** and **5**), and all these contacts were observed to lead to AFM interchain coupling. A strict application of the McConnell I model was not possible, in the case of the interchain contacts, as the shortest contacts would involve mediation through H or F atoms, which are expected to present a very small spin density. However, the results regarding the nature of the interchain magnetic coupling would be compatible with that model if the H or F atoms were neglected. The interchain magnetic coupling was estimated to decrease in the order $\mathbf{4 > 2 > 5 > 1 > 3}$. In these compounds metamagnetism

was only observed in case of **2** and **4**. In the other compounds a metamagnetic behavior is also expected to occur, but at lower temperatures ($T < 1.7$ K).

5. Supplementary material

Crystallographic data for the structural analysis have been deposited with the Cambridge Crystallographic Data Centre, CCDC Nos. 162843 and 162844 for compounds **1** and **2**, respectively. Copies of this information may be obtained free of charge from The director, CCDC, 12 Union Road, Cambridge, CB2 1EZ, UK (fax: +44-1223-336-033; e-mail: deposit@ccdc.cam.ac.uk or www: http://www.ccdc.cam.ac.uk).

Acknowledgements

This work was partially supported by 'Fundação para a Ciência e Tecnologia' under contracts PBIC/C/2204/95 and PRAXIS/P/QUI/12603/1998 from PRAXIS XXI program. The theoretical work in Barcelona was supported by grants of computer time by CESCA-CEPBA and also by the DGCYT and CIRIT (contracts # PB98-1166-C02-02 and 1999SGR-00046, respectively).

References

[1] (a) J.A. Candela, L.J. Swartzendruber, J.S. Miller, M.J. Rice, J. Am. Chem. Soc. 101 (1979) 2755;
(b) J.S. Miller, J.H. Zhang, W.M. Reiff, D.A. Dixon, L.D. Preston, A.H. Reis Jr., E. Gebert, M. Extine, J. Troup, A.J. Epstein, M.D. Ward, J. Phys. Chem. 91 (1987) 4344.

[2] (a) J.S. Miller, J.C. Calabrese, A.J. Epstein, W. Bigelow, J.H. Zhang, W.M. Reiff, J. Chem. Soc., Chem. Commun. (1986) 1026;
(b) S. Chittipeddi, K.R. Cromack, J.S. Miller, A.J. Epstein, Phys. Rev. Lett. 58 (1987) 2695.

[3] G.T. Yee, J.M. Manriquez, D.A. Dixon, R.S. McLean, D.M. Grosky, R.B. Flippen, K.S. Narayan, A.J. Epstein, J.S. Miller, Adv. Mater. 3 (1991) 309.

[4] (a) D.M. Eichhorn, D.C. Skee, W.E. Broderick, B.M. Hoffman, Inorg. Chem. 32 (1993) 491;
(b) J.S. Miller, R.S. McLean, C. Vasquez, F. Zuo, A.J. Epstein, J. Mater. Chem. 3 (1993) 215.

[5] W.E. Broderick, D.M. Eichhorn, X. Liu, P.J. Toscano, S.M. Owens, B.M. Hoffman, J. Am. Chem. Soc. 117 (1995) 3641.

[6] W.E. Broderick, J.A. Thompson, E.P. Day, B.M. Hoffman, Science 249 (1990) 401.

[7] W.E. Broderick, B.M. Hoffman, J. Am. Chem. Soc. 113 (1991) 6334.

[8] J.S. Miller, A.J. Epstein, in: C.J. O'Connor (Ed.), Research Frontiers in Magnetochemistry, World Science, Singapore, 1993, p. 283.

[9] H.M. McConnell, Proc. Robert A. Welch Found. Conf. Chem. Res. 11 (1967) 144.

[10] (a) C. Kollmar, M. Couty, O. Kahn, J. Am. Chem. Soc. 113 (1991) 7994;
(b) C. Kollmar, O. Kahn, J. Chem. Phys. 96 (1992) 2988.

[11] (a) O. Kahn, Molecular Magnetism, VCH, New York, 1993 (chap. 12);
(b) J.S. Miller, A.J. Epstein, Angew. Chem., Int. Ed. Engl. 33 (1994) 385.

[12] M. Deumal, J.J. Novoa, M.J. Bearpark, P. Celani, M. Olivucci, M.A. Robb, J. Phys. Chem. A 102 (1998) 8404.

[13] M. Deumal, J. Cirujeda, J. Veciana, J.J. Novoa, Chem. Eur. J. 5 (1999) 1631.

[14] J.S. Miller, J.C. Calabrese, A.J. Epstein, Inorg. Chem. 28 (1989) 4230.

[15] J.S. Miller, private communication.

[16] W.E. Broderick, J.A. Thompson, B.M. Hoffman, Inorg. Chem. 30 (1991) 2958.

[17] V. Gama, D. Belo, S. Rabaça, I.C. Santos, H. Alves, J.C. Waerenborgh, M.T. Duarte, R.T. Henriques, Eur. J. Inorg. Chem. (2000) 2101.

[18] D. Belo, H. Alves, S. Rabaça, L.C.J. Pereira, M.T. Duarte, V. Gama, R.T. Henriques, M. Almeida, E. Ribera, C. Rovira, J. Venciana, Eur. J. Inorg. Chem., in press.

[19] V. Gama, S. Rabaça, C. Ramos, D. Belo, I.C. Santos, M.T. Duarte, Mol. Cryst. Liq. Cryst. 335 (1999) 81.

[20] J.S. Miller, J.C. Calabrese, H. Rommelmann, S.R. Chittipeddi, J.H. Zhang, W.M. Reiff, A.J. Epstein, J. Am. Chem. Soc. 109 (1987) 769.

[21] W.B. Heuer, A.E. True, P.N. Swepston, B.M. Hoffman, Inorg. Chem. 27 (1988) 1474.

[22] G.M. Sheldrick, SHELXS-97, A Program for Crystal Structure Determination, University of Göttingen, Göttingen, Germany, 1990 (Acta Crystallogr., Sect. A 46 (1990) 467 for direct methods SHELXS-97).

[23] (a) G.M. Sheldrick, SHELXL-97, A Computer Program for Refinement of Crystal Structures, University of Göttingen, Göttingen, Germany, 1997;
(b) G.M. Sheldrick, T.R. Schneider, SHELXL, High-Resolution Refinement, in: C.W. Carter, R.M. Sweet (Eds.), Methods in Enzymology, vol. 277, Macromolecular Crystallography Part B, pp. 319–343.

[24] E. Keller, SCHAKAL-97, A Computer Program for the Representation of Molecular and Crystallographic Models, Kristallographisches Institut der Universität Freiburg i. Br., Germany, 1997.

[25] A.C.T. North, D.C. Philips, F.S. Mathews, Acta Cryst. A 24 (1968) 351.

[26] S. Rabaça, R. Meira, L.C.J. Pereira, M.T. Duarte, V. Gama, J. Organomet. Chem. 632 (2001) 67.

[27] S. Rabaça, R. Meira, L.C.J. Pereira, M.T. Duarte, V. Gama, in preparation.

[28] A.D. Becke, J. Chem. Phys. 98 (1993) 5648.

[29] P.J. Hay, W.R. Wadt, J. Chem. Phys. 82 (1985) 270.

[30] J. Blumel, N. Hebendanz, P. Hudeczek, F.H. Kohler, W. Strauss, J. Am. Chem. Soc. 114 (1992) 4223.

[31] A. Narath, Phys. Rev. 139 (1965) A1221.